J Fluoresc (2014) 24:933–943
DOI 10.1007/s10895-014-1374-3

ORIGINAL PAPER

Synthesis, Crystal Structures and Photo- and Electro-Luminescence of Copper(I) Complexes Containing Electron-Transporting Diaryl-1,3,4-Oxadiazole

Tianzhi Yu · Peng Liu · Haifang Chai · Jundan Kang · Yuling Zhao · Hui Zhang · Duowang Fan

Received: 21 October 2013 / Accepted: 3 March 2014 / Published online: 23 March 2014

Abstract Two mononuclear Cu(I) complexes based on 2-(2-pyridyl)benzimidazolyl derivative ligand containing electron-transporting 1,3,4-oxadiazole group (L), [Cu(**L**)$(PPh_3)_2$](BF_4) and [Cu(**L**)(DPEphos)](BF_4), where L = 1-(4-(5-(4-tert-butylphenyl)-1,3,4-oxadiazol-2-yl)benzyl)-2-(pyridin-2-yl)benzimidazole and DPEphos = bis[2-(diphenylphosphino)phenyl]ether, have been successfully synthesized and characterized. The X-ray crystal structure analyses of the ligand **L** and the complex [Cu(**L**)$(PPh_3)_2$](BF_4) were described. The photophysical properties of the complexes were examined by using UV–vis, photoluminescence spectroscopic analysis. The doped light-emitting devices using the Cu(I) complexes as dopants were fabricated. With no electron transporting layers employed in the devices, yellow electroluminescence from Cu(I) complexes were observed. The devices based on the complex [Cu(**L**)(DPEphos)](BF_4) possess better performance as compared with the devices fabricated by the complex [Cu(**L**)$(PPh_3)_2$](BF_4). The devices with the structure of ITO/MoO_3 (2 nm)/NPB (40 nm)/CBP:[Cu(**L**)(DPEphos)](BF_4) (8 wt%, 30 nm)/BCP (30 nm)/LiF (1 nm)/Al (150 nm) exhibit a maximum efficiency of 3.04 cd/A and a maximum brightness of 4,758 cd/m^2.

Keywords Copper(I) complex · Crystal structure · Benzimidazolyl derivative · Photoluminescence · Electroluminescence

T. Yu (✉) · P. Liu · H. Chai · H. Zhang · D. Fan
Key Laboratory of Opto-Electronic Technology and Intelligent Control (Ministry of Education), Lanzhou Jiaotong University, Lanzhou 730070, China
e-mail: yutianzhi@hotmail.com

P. Liu · H. Chai · J. Kang · Y. Zhao
School of Chemical and Biological Engineering, Lanzhou Jiaotong University, Lanzhou 730070, China

Introduction

Luminescent transition metal complexes have been extensively investigated due to their various applications ranging from organic light-emitting diodes (OLEDs) [1–3] and light emitting electrochemical cells (LEECs) [4, 5] to biological sensors [6–9]. By choosing appropriate metal ions and organic ligands, it is possible to control and coordinate the structures and the photonic properties of metal complexes.

Since Forrest and co-workers [10] successfully utilized the phosphorescent material PtOEP (platinum octaethylporphyrin) to fabricate light-emitting devices, many heavy-metal complexes have been extensively investigated in highly efficient electrophosphorescent organic light-emitting diodes [1, 11–14]. In the heavy-metal phosphorescent complexes, although Cu(I) complexes have relatively low quantum yields as compared with Ir(III) cyclometalated complexes, phosphorescent Cu(I) complexes have attracted much attention as a new class of optoelectronic materials in chemical sensors, probes of biological systems and OLEDs because of their advantages of less toxic, low cost, stable supply of copper metal and environmental friendliness [1, 10–14]. From previous publications, mono-, bi- and polynuclear Cu(I) acetylide complexes exhibited long-lived intense phosphorescence both in the solid state and solution, judicious selection of the acetylide group may be used to tune the emission wavelength across the vision spectrum from the blue to the red on substitution with increasingly electron-rich ligands [15, 16]. Recently, the heteroleptic $[Cu(N^N)(P^P)]^+$ complexes (where N^N and P^P denote a chelating bisimine ligand and a bisphosphine ligand, respectively) have attracted great attention because they exhibit greatly enhanced emission performance by the highly rigid and stronger metal-

phosphine bonding [17–21]. It has been shown that increased structural rigidity reduces radiationless deactivation pathways in mononuclear Cu(I) complexes leading to strongly enhanced quantum yields. For these Cu(I) complexes, the highest occupied molecular orbital (HOMO) has a predominant metal d character, possibly mixed with a small contribution from the bis-phosphine ligand, while the lowest unoccupied molecular orbital (LUMO) is essentially residing on the π* orbital localized on the bisimine ligand [22].

In recent years some examples have confirmed the suitability of such Cu(I) complexes as emitters in OLEDs [19, 22–27], but most Cu(I) complexes are unstable toward sublimation and poor soluble or unstable in solution and hence not amenable to the vacuum deposition or solution-processed methods used to fabricate OLEDs, few devices containing Cu(I) complexes have been reported. The strongly appealing possibility of using cheap Cu(I) complexes for replacing the more expensive complexes based on Ir(III) or other metal ions is still a challenge and under investigation.

In this work, two new mononuclear Cu(I) complexes containing electron-transporting 1,3,4-oxadiazole moiety, [Cu(**L**)(DPEphos)](BF_4) and [Cu(**L**)(PPh_3)$_2$](BF_4) (L= 1-(4-(5-(4-tert-butylphenyl)-1,3,4-oxadiazol-2-yl)benzyl)-2-(pyridin-2-yl)benzimidazole), were synthesized and characterized. The photophysical properties of the complexes were examined by using UV–vis, photoluminescence spectroscopes analysis. Furthermore, the devices made using codeposition of the Cu(I) complexes and 4,4′-Bis(9-carbazolyl)biphenyl (CBP) films as emitters were fabricated. The synthetic routes of the ligand (L) and the Cu(I) complexes were shown in Scheme 1.

Experimental Section

Materials and Methods

$Cu(BF_4)_2$•$6H_2O$, bis[2-(diphenylphosphino)phenyl]ether (DPEphos) were purchased from Aldrich. 2-(2-pyridyl)benzimidazole and triphenylphosphine (PPh_3) were obtained from Acros Organics. Copper powder was from Shenyang Keda Chemical Reagent Factory (China). Molybdenum trioxide (MoO_3), 4,4′-Bis(9-carbazolyl)biphenyl (CBP), N,N′-bis-(naphthyl)-N,N′-diphenyl-1,1′-biphenyl-4,4′-diamine (NPB) were purchased from Electro-Light Technology Corp., Beijing. Bathocuproine (BCP) was obtained from Sigma-Aldrich. All other chemicals were analytical grade reagent.

The intermediate, 2-[4-(Bromomethyl)phenyl]-5-(4-tertbutylphenyl)-1,3,4-oxadiazole (**I**), was obtained as previously described [28]. [Cu($NCCH_3$)$_4$](BF_4) was obtained by reaction of $Cu(BF_4)_2$•$6H_2O$ and copper powder in acetonitrile according to the method reported by Kubas [29].

IR spectra (400–4,000 cm^{-1}) were carried out using a Shimadzu IRPrestige-21 FT-IR spectrophotometer. ^1H NMR spectra were obtained on Unity Varian-500 MHz. Elemental analyses were obtained using an Elemental Vario-EL automatic elemental analysis instrument. Melting points were measured by using an X-4 microscopic melting point apparatus (Beijing Taike Instrument Limited Company). UV–vis absorption and photoluminescent spectra were recorded on a Shimadzu UV-2550 spectrometer and on a Perkin-Elmer LS-55 spectrometer, respectively. The electroluminescent spectra were measured on a PR-650 SpectraScan Colorimeter.

Synthesis and Characterization of 1-(4-(5-(4-Tert-Butylphenyl)-1,3,4-Oxadiazol-2-yl) Benzyl)−2-(Pyridin-2-yl)Benzimidazole (L)

Under N_2, solid NaH (60 % dispersed in mineral oil, 0.204 g) and 2-(2-pyridyl)benzimidazole (0.708 g, 3.65 mmol) in 20 mL of anhydrous DMF was stirred at 80 °C for 2 h. The resulting solution was cooled to room temperature and 2-[4-(Bromomethyl)phenyl]-5-(4-tertbutylphenyl)-1,3,4-oxadiazole (**I**) (1.68 g, 4.53 mmol) was added. The mixed solution was stirred at 80 °C for 36 h. After completing, the reaction mixture was poured into 100 mL of cool water, and was extracted with dichloromethane (3×50 mL). The organic phase was washed with water and dried over anhydrous $MgSO_4$. After removal of solvent, the residue was purified by column chromatography using ethyl acetate / petroleum ether (3 : 20, v/v) as the eluent to give a white powder (1.51 g, 85.8 %). m.p.:201–203 °C. IR (KBr pellet cm^{-1}): 3052 (Aryl-CH), 2966 and 2865(−CH_3, −CH_2–), 1617, 1589, 1494, 1441, 1426, 1388, 1364, 1326, 1263, 1168, 1073, 1020, 992, 834, 752. ^1H NMR($CDCl_3$, δ, ppm): 8.61 (d, 1H, *J*=5.4, Aryl-H), 8.47 (d, 1H, *J*=7.3, Aryl-H), 8.02 (t, 4H, J=8.8, Aryl-H), 7.90-7.83 (m, 2H, Aryl-H), 7.53 (d, 2H, *J*=6.8, Aryl-H), 7.36-28 (6H, m, Aryl-H), 6.27 (s, 2H, N-CH_2–), 1.37 (s, 9H, −CH_3). Anal. Calc. for $C_{31}H_{27}N_5O$ (%): C, 76.68; H, 5.60; N, 14.42. Found: C, 77.03; H, 5.51; N, 14.55.

Synthesis and Characterization of [Cu(L)(DPEphos)](BF_4) and [Cu(L)(PPh_3)$_2$](BF_4)

[Cu(L)(DPEphos)](BF_4) and [Cu(L)(PPh_3)$_2$](BF_4) were synthesized by following procedures described in the literatures

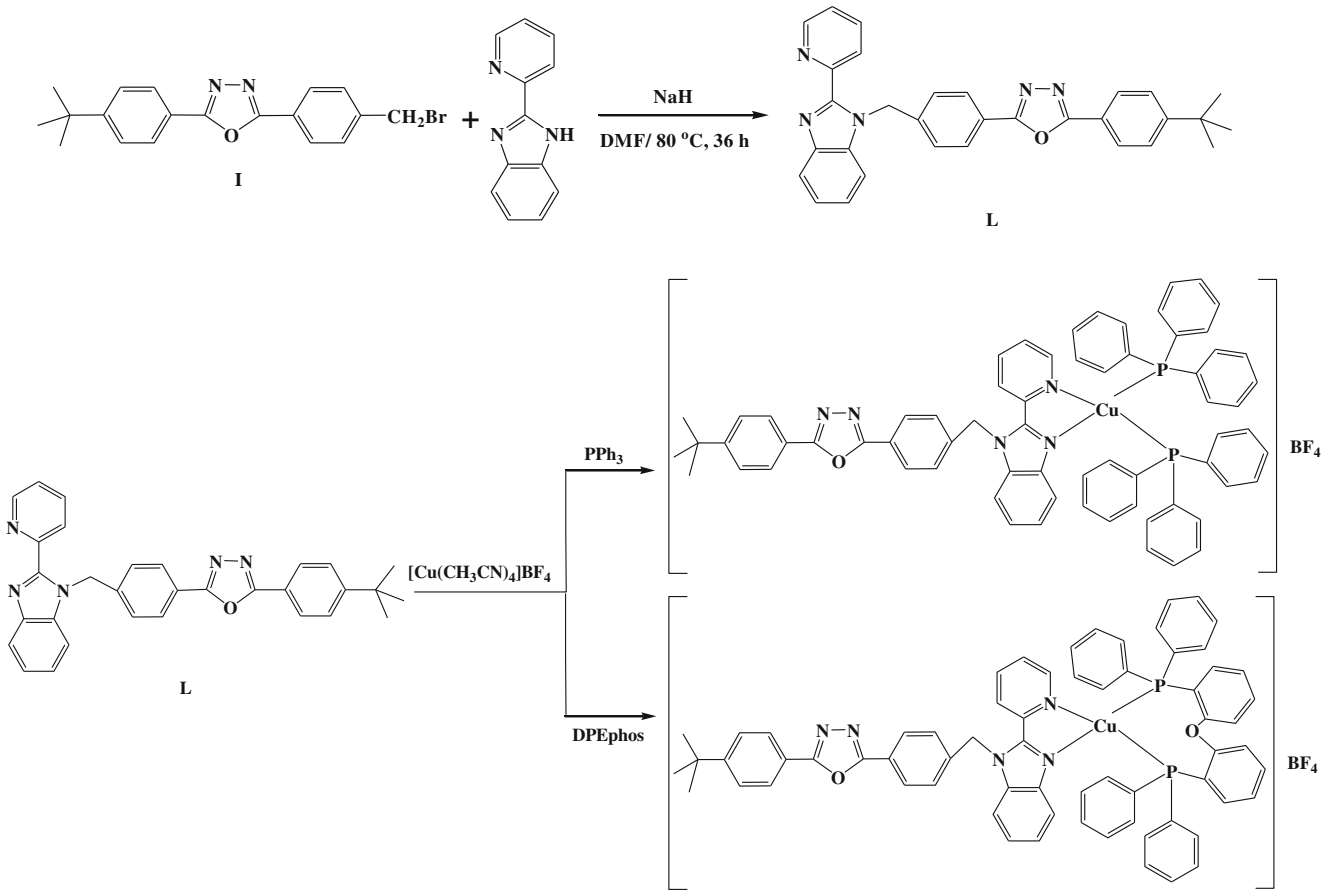

Scheme 1 Synthetic routes to the ligand (**L**) and the Cu(I) complexes

[30]. All manipulations were performed under a nitrogen atmosphere.

A mixture of $[Cu(NCCH_3)_4](BF_4)$ (1.0 mmol) and PPh_3 (2.0 mmol) or DPEphos (1.0 mmol) in anhydrous dichloromethane (10 mL) was stirred at room temperature for 1 h. 1-(4-(5-(4-tert-butylphenyl)-1,3,4-oxadiazol-2-yl)benzyl)-2-(pyridin-2-yl)benzimidazole (L) (1.0 mmol) in dichloromethane solution was added to the reaction mixture dropwise and stirring was continued for 12 h at room temperature to result in a clear yellow solution. The reaction mixture was concentrated to 5 mL, and hexane (15 mL) was then introduced to afford a yellow precipitate. The crude product was crystallized from toluene/hexane at ambient temperature to give air-stable, bright yellow crystals.

[Cu(L)(DPEphos)](BF4) Anal. Calc. for $C_{67}H_{55}N_5O_2P_2CuBF_4$ (%): C, 68.52; H, 4.72; N, 5.96. Found: C, 69.21; H, 4.65; N, 5.78. ^{1}H NMR($CDCl_3$, δ, ppm): 8.19 (d, 1H, *J*=4.8 Hz, Aryl-H), 8.09 (d, 2H, *J*= 8.4 Hz, Aryl-H), 8.04 (d, 2H, *J*=8.4, Aryl-H), 8.00-7.95 (m, 2H, Aryl-H), 7.54 (d, 2H, *J*=8.4 Hz, Aryl-H), 7.48 (d, 1H, *J*=8.4, Aryl-H), 7.39 (t, 4H, *J*=8.0, Aryl-H), 7.36-7.30 (m, 4H, Aryl-H), 7.26-7.11 (m, 16H, Aryl-H), 7.03-6.92 (m, 6H, Aryl-H), 6.86 (d, 4H, J=5.2, Aryl-H), 6.00 (s, 2H, N-CH_2–), 1.62 (s, 9H, −CH_3).

[Cu(L)(PPh3)2](BF4) Anal. Calc. for $C_{67}H_{57}N_5P_2OCuBF_4$ (%): C, 69.34; H, 4.95; N, 6.03. Found: C, 70.07; H, 5.06; N, 6.12. ^{1}H NMR($CDCl_3$, δ, ppm): 8.22 (d, 1H, *J*=5.2 Hz, Aryl-H), 8.13 (d, 1H, *J*=7.8 Hz, Aryl-H), 8.06 (t, 5H, *J*=5.6, Aryl-H), 7.54 (t, 2H, *J*=8.4, Aryl-H), 7.47 (d, 1H, *J*=9.6 Hz, Aryl-H), 7.42 (t, 1H, *J*=6.8 Hz, Aryl-H), 7.36 (t, 7H, *J*=7.2, Aryl-H), 7.29 (t, 4H, *J*=8.4 Hz, Aryl-H), 7.18 (t, 12H, *J*= 7.6 Hz, Aryl-H), 7.11 (d, 12H, *J*=7.2 Hz, Aryl-H), 6.09 (s, 2H, N-CH_2–), 1.37 (t, 9H , −CH_3).

Crystallography

The diffraction data were collected with a Bruker Smart Apex CCD area detector with graphite-monochromatized Mo-Kα radiation (λ=0.71073 Å) at 188(2) K. The structure was solved by using the program SHELXL and Fourier difference techniques, and refined by full-

matrix least-squares method on F^2. All hydrogen atoms were added theoretically.

OLEDs Fabrication and Characterization

The multilayer OLEDs with a device architecture of ITO/MoO_3 (2 nm)/NPB (40 nm)/CBP:Cu(I) complex (x wt %, 30 nm)/BCP (30 nm)/LiF (1 nm)/Al (150 nm) were fabricated by vacuum-deposition method. All organic layers were sequentially deposited without breaking vacuum (2×10^{-5} Pa). Thermal deposition rates for organic materials, LiF and Al were~2 Å/s, ~ 1 Å/s and 10 Å/s, respectively. The active area of the devices was 12 mm^2. The EL spectra and Commission Internationale de L'Eclairage (CIE) coordinates were measured on a Hitachi MPF-4 fluorescence spectrometer. The characterization of brightness-current–voltage (B–I–V) were measured with a 3,645 DC power supply combined with a 1980A spot photometer and were recorded simultaneously. All measurements were done in air at room temperature without any encapsulation.

Results and Discussion

Syntheses of the Ligand L and the Cu(I) Complexes

The ligand **L** was obtained by reaction of the intermediate **I** with 2-(2-pyridyl)benzimidazole in the presence of NaH as a base. The ligand **L** was fairly soluble in most common solvents, such as MeOH, CH_2Cl_2, $CHCl_3$ and EtOAc. The ligand **L** was fully characterized by elemental analysis, ^{1}H NMR, FT-IR and X-ray single crystal analysis.

The Cu(I) complexes [Cu(**L**)(DPEphos)](BF_4) and [Cu(**L**)(PPh_3)$_2$](BF_4) were obtained by reaction of [Cu($NCCH_3$)$_4$](BF_4) with **L** and different ancillary

Table 1 Crystallographic data for the Ligand **L** and the Cu(I) complex

Compound	L	[Cu(L)(PPh_3)$_2$](BF_4)•2CH_2Cl_2
Empirical formula	$C_{31}H_{27}N_5O$	$C_{69}H_{61}N_5P_2OCuBF_4Cl_4$
Formula weight	485.58	1330.32
Temperature (K)	188(2)	185(2)
Wavelength (Å)	0.71073	0.71073
Crystal system	Triclinic	Triclinic
Space group	P-1	P-1
Unit cell dimensions		
a (Å)	6.2430(7)	15.0070(8)
b (Å)	9.7305(11)	20.7612(11)
c (Å)	20.938(2)	22.8166(12)
α (°)	92.008(2)	101.8768(8)
β (°)	94.428(2)	105.9971(8)
γ (°)	94.767(2)	100.3098(7)
Volume ($Å^3$), Z	1262.6(2), 2	6473.9(6), 4
Density (calculated) (g/cm^3)	1.277	1.365
Absorption coefficient (mm^{-1})	0.080	0.611
F (000)	512	2744
Crystal size (mm)	0.39×0.28×0.20	0.32×0.24×0.11
θ range for data collected (°)	1.95 ─ 26.02	1.59 ─ 26.02
Limiting indices	−7≤h≤7, −11≤k≤11, −25≤l≤24	−18≤h≤16, −25≤k≤25, −25≤l≤28
Reflections collected	7867	41508
Independent reflections	4821 (R_{int}=0.0203)	24966 (R_{int}=0.0197)
Max. and min. transmission	0.9842 and 0.9695	0.9358 and 0.8285
Data / restraints / parameters	4821 / 0 / 337	24966 / 0 / 1573
Goodness-of-fit on F^2	1.020	1.024
Final R indices [I>2σ (I)]	R_1=0.0549, wR_2=0.1283	R_1=0.0533, wR_2=0.1362
R indices (all data)	R_1=0.0814, wR_2=0.1436	R_1=0.0761, wR_2=0.1517
Largest diff. Peak and hole ($eÅ^{-3}$)	0.264 and −0.201	0.768 and −0.714

Table 2 Selected interatomic distances (Å) and angles (°) of **L** and the Cu(I) complex

Ligand **L**			
C(1) – N(1)	1.389(3)	C(17) – N(4)	1.435(3)
C(6) – N(2)	1.392(3)	C(20) – N(4)	1.292(3)
C(7) – N(2)	1.319(3)	C(21) – N(5)	1.293(3)
C(7) – N(1)	1.376(2)	C(20) – O(1)	1.362(2)
C(8) – N(3)	1.334(3)	C(21) – O(1)	1.368(2)
C(12) – N(3)	1.346(3)	N(4) – N(5)	1.410(2)
C(13) – N(1)	1.465(2)		
C(2)–C(1)-N(1)	131.52(19)	C(7)-N(1)–C(1)	105.87(16)
C(6)–C(1)-N(1)	105.98(18)	C(7)-N(1)–C(13)	131.08(16)
C(5)–C(6)-N(2)	130.52(19)	C(1)-N(1)–C(13)	122.73(16)
C(1)–C(6)-N(2)	109.73(18)	C(7)-N(2)–C(6)	104.98(16)
N(1)–C(7)-N(2)	113.43(18)	C(8)-N(3)–C(12)	116.5(2)
N(2)–C(7)–C(8)	120.81(18)	N(3)–C(8)–C(7)	118.62(18)
N(1)–C(7)–C(8)	125.76(18)	N(3)–C(12)–C(11)	124.0(3)
N(3)–C(8)–C(9)	122.6(2)	N(1)–C(13)-C(14)	112.76(16)
$[Cu(L)(PPh_3)_2](BF_4)•2CH_2Cl_2$			
Cu(1) – N(1)	2.115(2)	Cu(2) – N(6)	2.124(2)
Cu(1) – N(2)	2.038(2)	Cu(2) – N(7)	2.048(2)
Cu(1) – P(1)	2.2630(8)	Cu(2) – P(3)	2.2424(8)
Cu(1) – P(2)	2.2552(8)	Cu(2) – P(4)	2.2544(8)
N(1)-Cu(1)-N(2)	78.55(9)	N(7)-Cu(2)-N(6)	79.33(9)
N(2)-Cu(1)-P(2)	113.94(7)	N(7)-Cu(2)-P(3)	113.07(7)
N(1)-Cu(1)-P(2)	115.96(7)	N(6)-Cu(2)-P(3)	114.89(7)
N(2)-Cu(1)-P(1)	114.60(7)	N(7)-Cu(2)-P(4)	112.40(7)
N(1)-Cu(1)-P(1)	104.29(6)	N(6)-Cu(2)-P(4)	103.92(7)
P(2)-Cu(1)-P(1)	121.27(3)	P(3)-Cu(2)-P(4)	124.09(3)

phosphoric ligands (PPh_3 and DPEphos) in anhydrous dichloromethane. The Cu(I) complexes were also examined by elemental analysis, ^1H NMR. The structure of $[Cu(\mathbf{L})(PPh_3)_2](BF_4)$ was characterized by X-ray single crystal analysis.

X-ray Crystal Structure of the Ligand L and the Complex $[Cu(L)(PPh_3)_2](BF_4)$

Suitable crystal of the ligand **L** was obtained by evaporation of ethyl acetate solution. Suitable crystal of $[Cu(\mathbf{L})(PPh_3)_2](BF_4)$ complex was obtained by the vapor diffusion of diethyl ether into the dichloromethane solution of the Cu(I) complex, it is yellow crystal. The crystallographic data of **L** and $[Cu(\mathbf{L})(PPh_3)_2](BF_4)$ are shown in Table 1. The selected bond lengths and bond angles of **L** and $[Cu(\mathbf{L})(PPh_3)_2](BF_4)$ are listed in Table 2.

The crystal structure and packing diagram of **L** are given in Fig. 1. As shown in Fig. 1a, the pyridyl ring and benzimidazole ring of 2-(2-pyridyl)benzimidazole moiety is not in a plane, the dihedral angel of them is 19.9°. In diaryl-1,3,4-oxadiazole moiety, the 1,3,4-oxadiazole ring and two adjacent phenyl rings are not also in a coplane, and the dihedral angels between the 1,3,4-oxadiazole ring and two adjacent phenyl rings are 8.6° and 10.1°, respectively. The dihedral angels between benzyl ring and the pyridyl ring and benzimidazole ring of 2-(2-pyridyl)benzimidazole moiety are 78.6° and 74.4°, respectively. From the packing diagram of **L** (Fig. 1b), there are weak intermolecular π-π interactions between the 2-(2-pyridyl)benzimidazole skeletons of two adjacent molecules along *b*-axis in crystal lattices, the interplanar distance of the 2-(2-pyridyl)benzimidazole skeletons is approximately 3.69 Å.

Figure 2 gives the crystal structure of $[Cu(\mathbf{L})(PPh_3)_2](BF_4)$ complex. It indicates that the asymmetric unit of $[Cu(\mathbf{L})(PPh_3)_2](BF_4)$ complex consists of two crystallographic-separate complexes and four dichloromethane molecules. Thus, the crystal of the Cu(I) complex suitable for X-ray analysis was described as the solvate species $2[Cu(\mathbf{L})(PPh_3)_2](BF_4)•4CH_2Cl_2$. As shown in Fig. 2, the coordination center of Cu atom is surrounded by two N atoms from **L** ligand and two P atoms from two PPh_3 ligands, displaying distorted tetrahedral coordination geometry. The intersection angle of N(1)-Cu(1)-N(2) and P(1)-Cu(1)-P(2) planes is as large as 84.4°, and the N(1)-Cu(1)-N(2) and P(1)-Cu(1)-P(2) bond angles are 78.55 (9)° and 121.27 (3)°, respectively. The two Cu-P (Cu(1)-P(1) and Cu(1)-P(2)) bond lengths are 2.2630 (8) and 2.2552 (8) Å, respectively. The Cu(1)-N(1) (pyridyl) bond length (2.115 (2) Å) is longer than the Cu(1)-N(2) (imidazolyl) bond length (2.038 (2) Å), which means that the intermolecular attraction between Cu(I) center and N (imidazolyl) is stronger than that between Cu(I) center and N (pyridyl). The N(7)-Cu(2)-N(6) and P(3)-Cu(2)-P(4) bond angles are 79.33 (9)° and 124.09 (3)°, respectively.

For the chelated ligand **L** in the crystal, the dihedral angle between the pyridyl ring and the benzimidazolyl ring is 3.5°, which is smaller than that of them in free Ligand **L** (19.9°). It suggests that the plane of pyridyl ring and the plane of benzimidazole ring takes place slight distortion and goes to be a coplane due to coordination of two N atoms to the Cu center atom.

Owing to highly disordered effect of the phenyl rings of PPh_3 ligands and steric hindrance of diaryl-1,3,4-oxadiazole moiety of ligand **L**, there is no intermolecular or inner molecular π-π stacking interaction in the crystal lattice.

UV–vis Absorption and Photoluminescence of the Cu(I) Complexes

The UV–vis absorption spectra of dilute dichloromethane solutions of the Cu(I) complexes and the free ligands are shown in Fig. 3. The absorption spectra of free DPEphos and PPh_3 are similar, exhibiting two absorption bands at 234

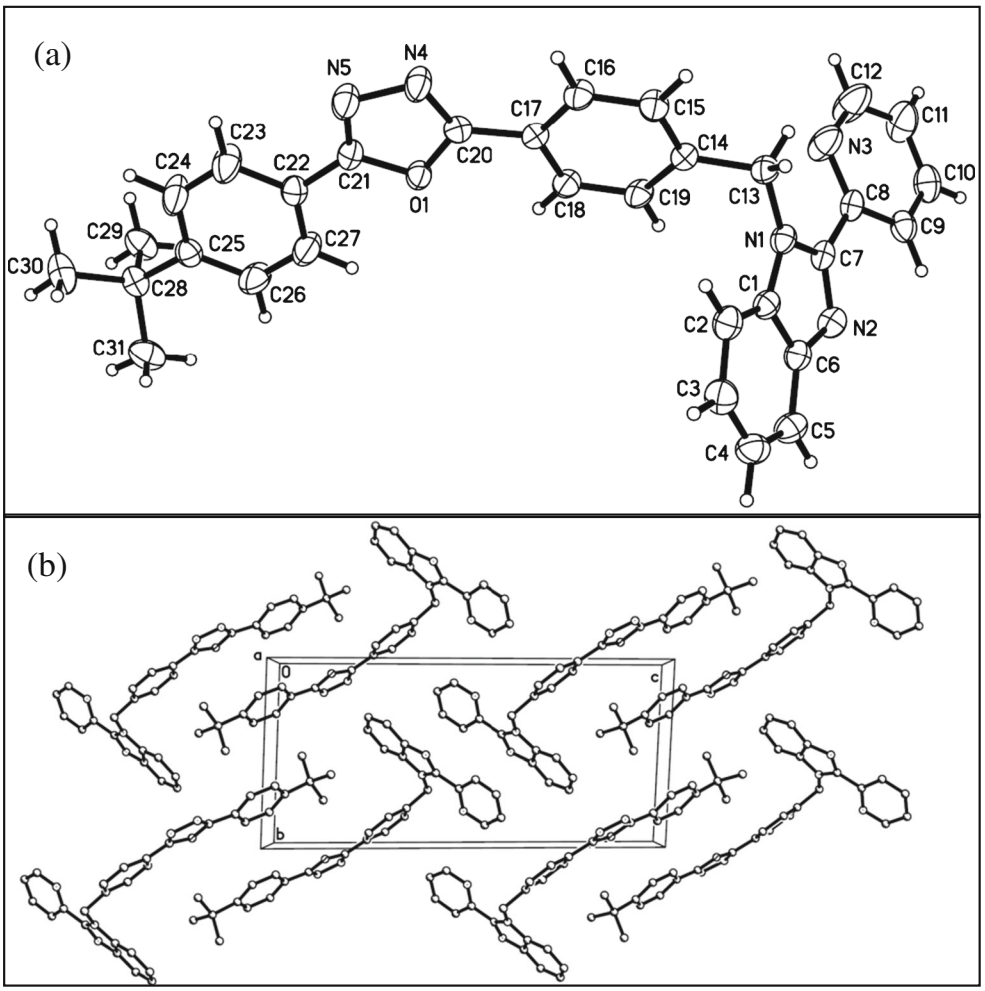

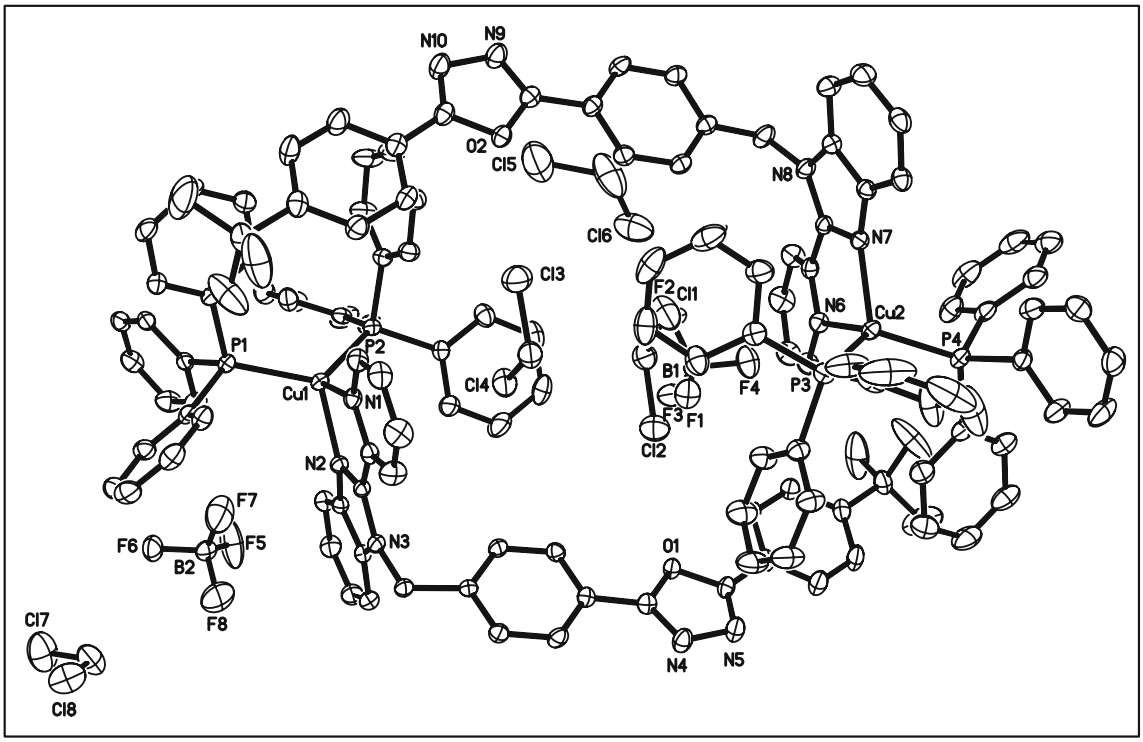

Fig. 1 Crystal structure (**a**) and packing diagram (**b**) of the ligand **L**

Fig. 2 Crystal structure of $[Cu(L)(PPh_3)_2](BF_4)$ complex

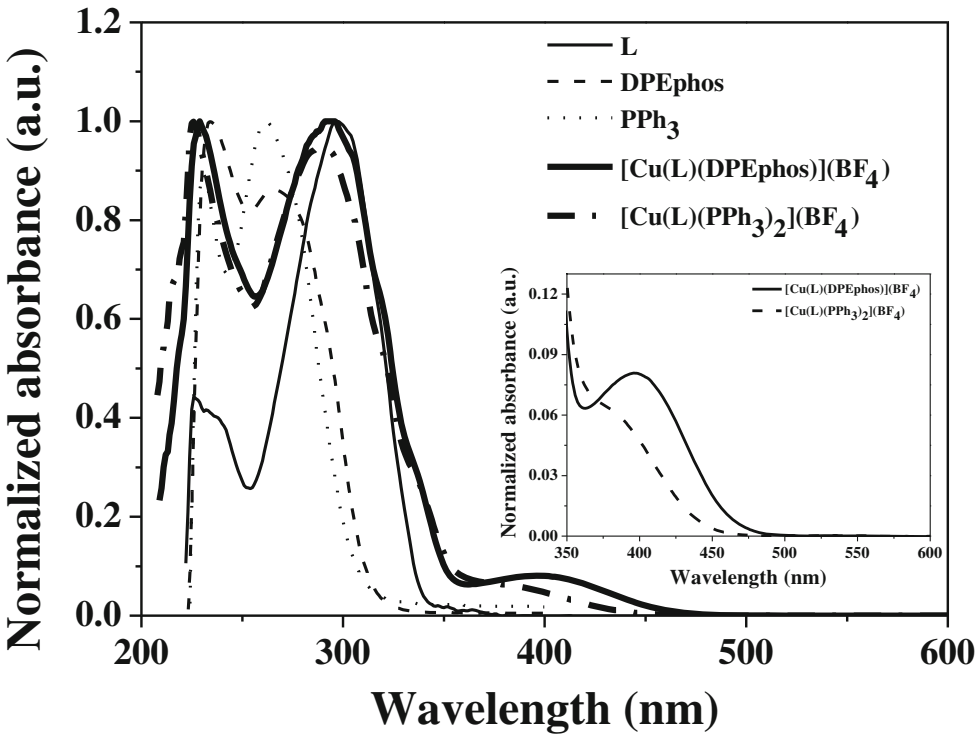

Fig. 3 Absorption spectra of free ligands and the Cu(I) complexes in dichloromethane solutions at room temperature. The inset shows a magnified view of the absorption edges for the Cu(I) complexes. ($C=1\times10^{-5}$ mol/L)

and 260 nm. The free ligand **L** has two intensive absorption bands at 228 and 297 nm, respectively. The absorption spectra of the complexes [Cu(**L**)(DPEphos)](BF_4) and [Cu(**L**)(PPh_3)$_2$](BF_4) strongly resemble each other, which can be described as two components: an intense absorption region in high energy band ranging from 220 to 360 nm and a weak absorption region in low energy band ranging from 360 to 480 nm. In intense absorption region, there are two visible absorption peaks at 229 and 294 nm. Comparing with the absorption spectra of free ligands, the high energy absorption bands of the complexes are found to be quite similar to those of free ligands and thus attributed to the $\pi\rightarrow\pi^*$ transitions of

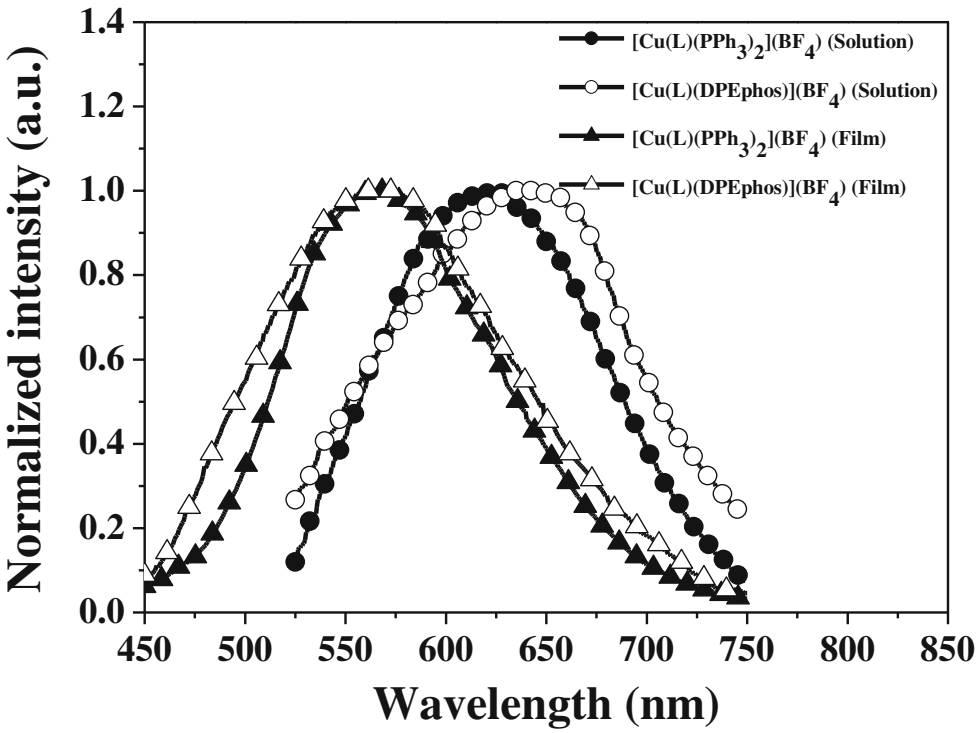

Fig. 4 Photoluminescent spectra of [Cu(L)(DPEphos)](BF_4) and [Cu(L)(PPh_3)$_2$](BF_4) in dichloromethane solutions and in thin films at room temperature. ($C=1\times10^{-5}$ mol/L, λ_{ex}=410 nm, slit widths are 5 nm)

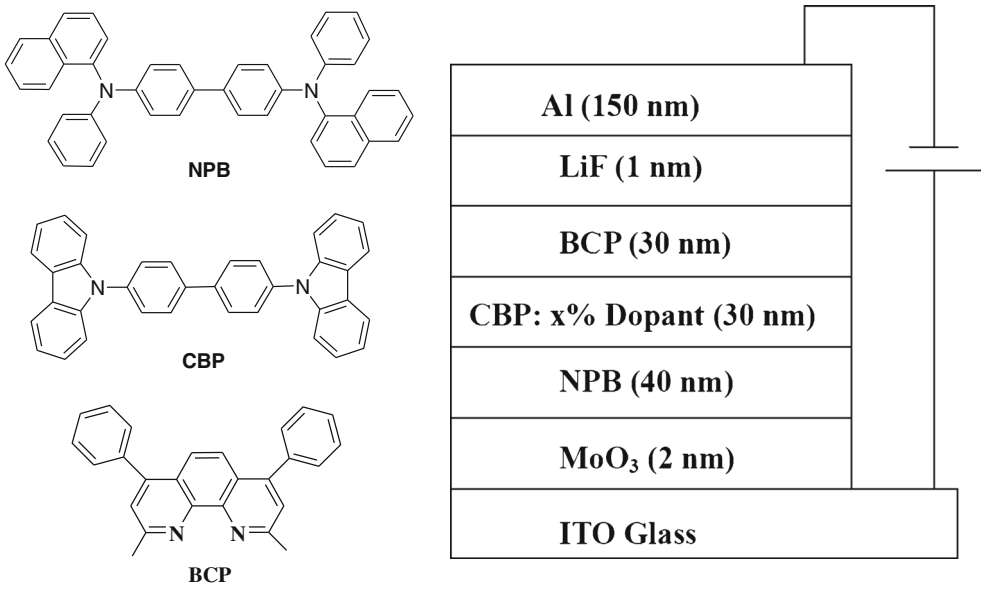

Fig. 5 The molecular structures of materials and the structure of EL devices

the ligands. The weak absorption band of the complex [Cu(**L**)(DPEphos)](BF_4) or [Cu(**L**)(PPh_3)$_2$](BF_4), which is a newly generated one compared with those of free ligands, is assigned to metal-to-ligand charge-transfer (MLCT) transitions [18, 31].

Influences of different environments on the emission properties of the complexes have been investigated. Ambient temperature emission spectra of the thin films and the dichloromethane solutions are shown in Fig. 4. It is found that the photoluminescence spectra of the complexes [Cu(**L**)(DPEphos)](BF_4) and [Cu(**L**)(PPh_3)$_2$](BF_4) strongly resemble each other. The emission spectra of the complexes are relatively broad and featureless whether in thin films or in dichloromethane solutions, which are assigned to the dπ(Cu)→π*(diimine) (^{3}MLCT) excited state, it suggests that the emissive states have a charge-transfer character [32]. The emission maxima for [Cu(**L**)(DPEphos)](BF_4) and [Cu(**L**)(PPh_3)$_2$](BF_4) as thin films locate at 568 nm, while the maxima are significantly red-shifted when measured in dichloromethane solutions exhibiting maxima at 638 and 620 nm, respectively. The result shows that the emission wavelengths strongly depend on the environment of the complexes. The observation can be explained by changes of the molecular geometry of the Cu(I) complexes which take place after MLCT excitation. In dichloromethane solutions, large rearrangements of the molecular geometry upon excitation can take place easily, which enhance radiationless deactivation processes leading to a considerable decrease of emission quantum yields. Similar phenomena have already been reported for several Cu(I) complexes [33, 34].

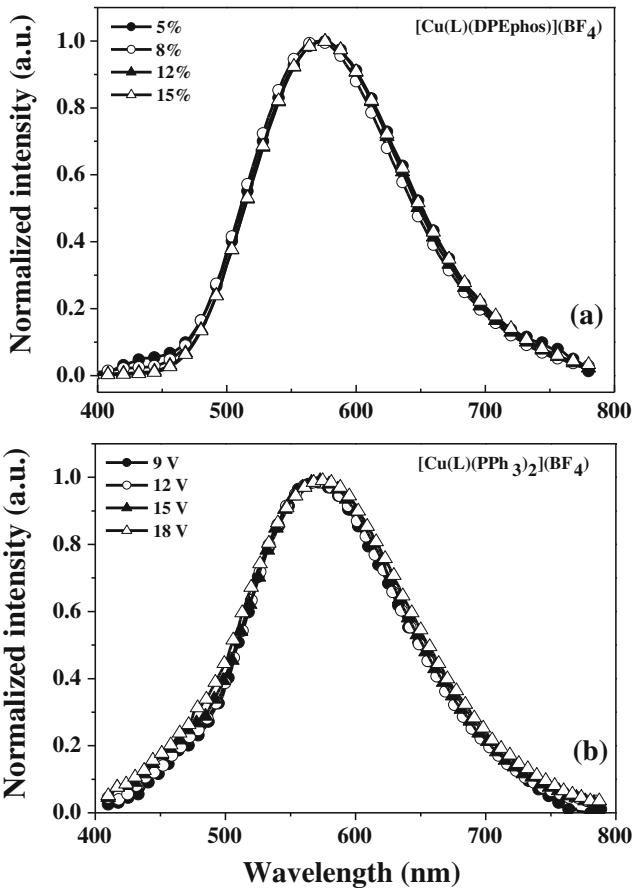

Fig. 6 EL spectra of the devices with various [Cu(L)(DPEphos)](BF_4) concentrations at applied voltage 8 V (**a**) and EL spectra of the devices used [Cu(L)(PPh_3)$_2$](BF_4) as a dopant (15 wt%) at different applied voltages (**b**)

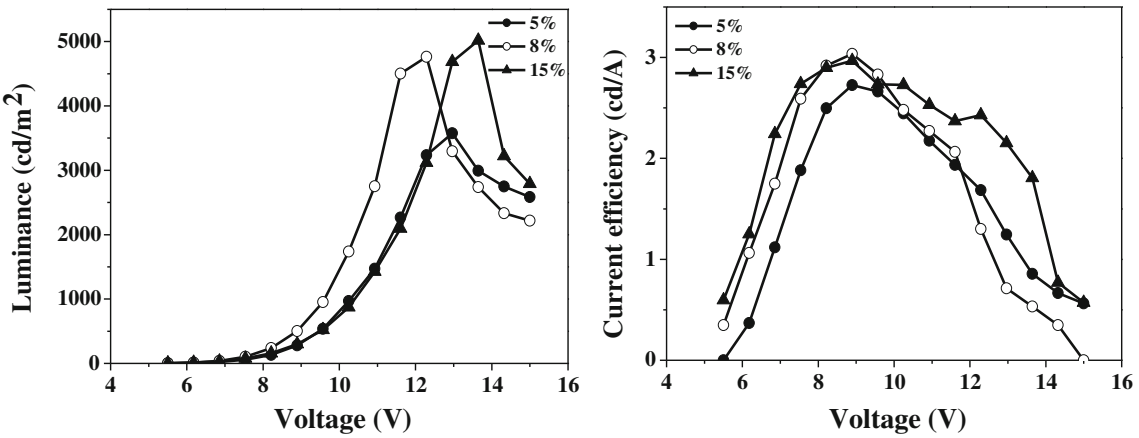

Fig. 7 The luminance vs. voltage (*left*) and current efficiency vs. voltage (*right*) curves of the devices with different [Cu(L)(DPEphos)](BF_4) concentrations

OLEDs Performance of [Cu(L)(DPEphos)](BF_4) and [Cu(L)(PPh_3)$_2$](BF_4)

The molecular structures of the materials and the devices with a configuration of ITO/MoO_3 (2 nm)/NPB (40 nm)/CBP:Cu(I) complex (x wt%, 30 nm)/BCP (30 nm)/LiF (1 nm)/Al (150 nm) were depicted in Fig. 5. The emitting layers are consisted of host materials CBP and dopants of the complexes [Cu(**L**)(-DPEphos)](BF_4) or [Cu(**L**)(PPh_3)$_2$](BF_4) at different concentrations (x wt%). MoO_3 and NPB were used as hole injection and hole transport materials, respectively. Bathocuproine (BCP) acts as the exciton blocking, and LiF was used as the electron-injection layer.

Figure 6 shows the electroluminescent (EL) spectra of the devices with various [Cu(**L**)(DPEphos)](BF_4) concentrations at applied voltage 8 V and EL spectra of the devices used [Cu(**L**)(PPh_3)$_2$](BF_4) as dopant (15 wt%) at different applied voltages. It was found that the EL spectral features of the devices used [Cu(**L**)(DPEphos)](BF_4) or [Cu(**L**)(PPh_3)$_2$](BF_4) as dopants do not change with different concentrations or different applied voltages. As shown in Fig. 6. no emission from the host CBP was found in EL spectra, indicating that charge trap occurred in the device operation beside the energy-transfer process. The doped devices of [Cu(**L**)(DPEphos)](BF_4) and [Cu(**L**)(PPh_3)$_2$](BF_4) exhibit yellow emissions with the maximum peaks at ca. 570 nm. The EL spectra of [Cu(**L**)(DPEphos)](BF_4) and [Cu(**L**)(-PPh_3)$_2$](BF_4) are identical to the PL spectra of them in thin films. The result indicates that the EL emissions take place from [Cu(**L**)(DPEphos)](BF_4) and [Cu(**L**)(PPh_3)$_2$](BF_4) molecules.

The electroluminescent devices with different doping concentrations varying from 5, 8 and 15 wt% were fabricated. The representative luminance voltage and current efficiency voltage characteristics of the devices doped [Cu(**L**)(-DPEphos)](BF_4) with different concentrations are depicted in Fig. 7. and the data of OLEDs performance are listed in Table 3. As shown in Table 3, the current efficiencies of the devices increase to the highest with increasing the concentration to 8 wt%, and further enhancement of the concentration results in reduction of the current efficiency. The turn-on voltages of the devices are between 6.0 V and 6.8 V, and the maximum brightness is between 3,586 cd/m^2 and 5,048 cd/m^2. By comparing the performance of different doping concentrations, the 8 wt% [Cu(**L**)(DPEphos)](BF_4) doped device has a maximum efficiency of 3.04 cd/A at 1.65 mA/cm^2, which has a yellow color with a CIE_{xy} of (0.45, 0.48). Even at 10 mA/cm^2, the doped device has a maximum efficiency of 2.35 cd/A. The device shows a turn-on voltage of about 6.5 V, the maximum brightness is about 4,758 cd/m^2 at 12.3 V.

Table 3 EL performances of the OLEDs based on Cu(I) complexes

Complex	Doped concentration (wt%)	Maximum efficiency (cd/A)	Efficiency at 10 mA/cm^2 (cd/A)	Maximum brightness (cd/m^2)	Emission wavelength (nm)
[Cu(L)(DPEphos)](BF_4)	5 %	2.73	2.02	3,586	570
	8 %	3.04	2.35	4,778	571
	15 %	2.98	2.39	5,048	573
[Cu(L)(PPh_3)$_2$](BF_4)	15 %	0.47	0.38	575	570

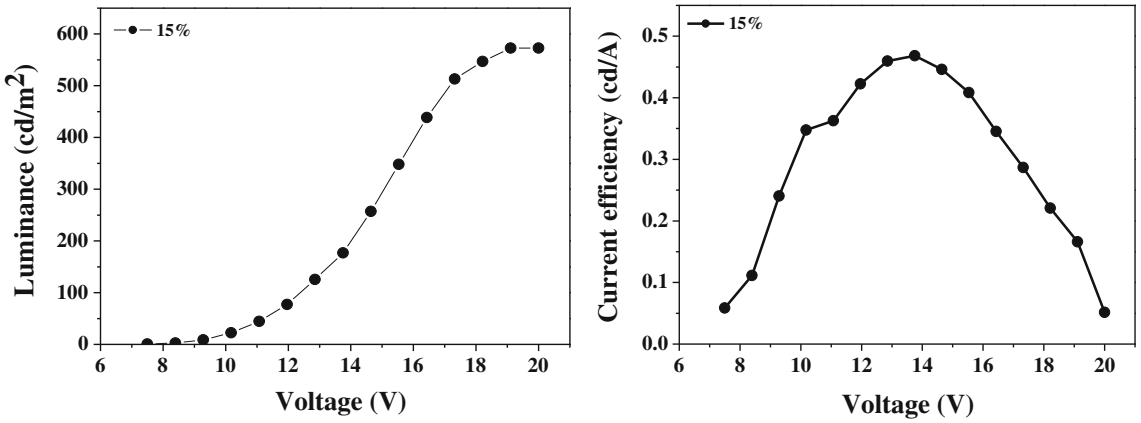

Fig. 8 The luminance vs. voltage (*left*) and current efficiency vs. voltage (*right*) curves of the device used [Cu(L)$(PPh_3)_2$](BF_4) as a dopant (15 wt%)

For [Cu(**L**)$(PPh_3)_2$](BF_4) complex, the EL performances of devices with different doping concentrations varying from 5, 8 and 15 wt% were also investigated, in which only the device with a doping concentration of 15 wt% can normally work. The luminance voltage and current efficiency voltage characteristics of the device doped [Cu(**L**)$(PPh_3)_2$](BF_4) concentration of 15 wt% are shown in Fig. 8. and the data of OLEDs performance are listed in Table 3. The device with a turn-on voltage of 8.3 V, maximum current efficiency of 0.47 cd/A, maximum brightness of 575 cd/m2 has been observed.

As shown in Table 3, we can see that the ancillary ligands play a significant impact on the EL performances of the Cu(I) complexes. Compared with the devices based on [Cu(**L**)(-DPEphos)](BF_4) complex, the device made from [Cu(**L**)(-$PPh_3)_2$](BF_4) complex exhibits much poorer EL performance. Compared to the monodentate ligand PPh_3, DPEphos is a bidentate ligand, causing larger molecular rigidity for [Cu(**L**)(DPEphos)](BF_4). Moreover, the chelate DPEphos ligand may increase the emission quantum efficiency and short the decay lifetime of [Cu(**L**)(DPEphos)](BF_4) [27].

From the configuration of the devices, though no electron transporting layers designedly employed in the devices, yellow EL emissions were observed from the devices used the Cu(I) complexes as dopants. It indicates that [Cu(**L**)(-DPEphos)](BF_4) and [Cu(**L**)$(PPh_3)_2$](BF_4) complexes have definite electron transporting ability because the ligand **L** was incorporated a diaryl-1,3,4-oxadiazole moiety, which validates our primal idea for the ligand **L**.

From the above results, we can see that the EL performances of the devices based on the cationic Cu(I) complexes were undesirable. The poorer EL performances may be caused by some factors such as the longer decay lifetime, unbalance of the charge carrier and the increased current density which was caused by the drifting and accumulating of BF_4^- counterions towards the anode (ITO) upon application of a bias, injection and so on. The longer decay lifetimes of the Cu(I) complexes based on 2-(2′-pyridyl)benzimidazolyl ligand are their intrinsic property [18], which decrease the emission quantum efficiency. If the appropriate hole and electron transporting materials are chosen, improving the charge carrier injection balance in the devices, we should obtain much better EL performances. Further investigation on the EL properties of the Cu(I) complexes are in progress.

Conclusion

A new 2-(2′-pyridyl)benzimidazole ligand (**L**) in which 2-(2′-pyridyl)benzimidazole is linked to a diaryl-1,3,4-oxadiazole moiety by a methylene spacer and two new mononuclear Cu(I) complexes, [Cu(**L**)(DPEphos)](BF_4) and [Cu(**L**)(-$PPh_3)_2$](BF_4), were successfully synthesized and characterized. The single crystal X-ray diffraction study of [Cu(**L**)(-$PPh_3)_2$](BF_4) reveals that the center Cu(I) ion assumes highly distorted tetrahedral geometry. Both the emission wavelengths as well as photoluminescence intensity strongly depend on the environment of the complexes as neat films and in solutions. The Cu(I) complexes are stable enough to be sublimated during EL device fabrication. At no electron transporting layers employed in the devices, yellow EL emissions were observed from the devices used the Cu(I) complexes as dopants. The devices fabricated by the complex [Cu(**L**)(DPEphos)](BF_4) possess better performance as compared with the devices fabricated by the complex [Cu(**L**)$(PPh_3)_2$](BF_4). When the doping concentration is 8 wt%, the doped devices based on [Cu(**L**)(DPEphos)](BF_4) demonstrate a CIE_{xy} of (0.45, 0.48) with a maximum efficiency of 3.04 cd/A at 1.65 mA/cm^2 and a maximum brightness of 4,758 cd/m^2 at 12.3 V.

Acknowledgments This work was supported by the Science and Technology Project of Lanzhou (2009-1-15), and also supported by the Program for Changjiang Scholars and Innovative Research Team in University (IRT0629).

References

1. Xiao LX, Chen ZJ, Qu B, Luo JX, Kong S, Gong QH, Kido J (2011) Recent progresses on materials for electrophosphorescent organic light-emitting devices. Adv Mater 23:926–952
2. Hudson ZM, Sun C, Helander MG, Amarne H, Lu ZH, Wang S (2010) Enhancing phosphorescence and electrophosphorescence efficiency of cyclometalated Pt(II) compounds with triarylboron. Adv Funct Mater 20:3426–3439
3. Borek C, Hanson K, Djurovich PI, Aznavour ME, Bau R, Sun Y, Forrest SR, Brooks J, Michalski L, Brown J (2007) Highly efficient, near-infrared electrophosphorescence from a Pt–metalloporphyrin complex. Angew Chem Int Ed 46:1109–1112
4. Wu C, Chen HF, Wong KT, Thompson ME (2010) Study of ion-paired iridium complexes (soft salts) and their application in organic light emitting diodes. J Am Chem Soc 132:3133–3139
5. Kapturkiewicz A (2010) Electrochemiluminescent systems as devices and sensors. In: Ceroni P, Credi A, Venturi M (eds) Electrochemistry of functional supramolecular systems. John Wiley & Sons, Hoboken
6. Lo KKW, Louie MW, Zhang KY (2010) Design of luminescent iridium(III) and rhenium(I) polypyridine complexes as in vitro and in vivo ion, molecular and biological probes. Coord Chem Rev 254: 2603–2622
7. Zhao Q, Li FY, Huang CH (2010) Phosphorescent chemosensors based on heavy-metal complexes. Chem Soc Rev 39:3007–3030
8. Yu MX, Zhao Q, Shi LX, Li FY, Zhou ZG, Yang H, Yi T, Huang CH (2008) Cationic iridium(III) complexes for phosphorescence staining in the cytoplasm of living cell. Chem Commun 2115–2117. doi:10.1039/B800939B
9. Botchway SW, Charnley M, Haycock JW, Parker AW, Rochester DL, Weinstein JA, Gareth Williams JA (2008) Time-resolved and two-photon emission imaging microscopy of live cells with inert platinum complexes. Proc Natl Acad Sci U S A 105:16071–16076
10. Baldo MA, O'Brien DF, You Y, Shoustikov A, Sibley S, Thompson ME, Forrest SR (1998) Highly efficient phosphorescent emission from organic electroluminescent devices. Nature 395:151–154
11. Thompson M (2007) The evolution of organometallic complexes in organic light-emitting devices. MRS Bull 32:694–701
12. You Y, Park SY (2009) Phosphorescent iridium(III) complexes: toward high phosphorescence quantum efficiency through ligand control. Dalton Trans 1267–1282. doi:10.1039/B812281D
13. Chou PT, Chi Y (2007) Phosphorescent dyes for organic light-emitting diodes. Chem Eur J 13:380–395
14. Evans RC, Douglas P, Winscom CJ (2006) Coordination complexes exhibiting room-temperature phosphorescence: evaluation of their suitability as triplet emitters in organic light emitting diodes. Coord Chem Rev 250:2093–2126
15. Yam VW-W, Lo KK-W, Wong KM–C (1999) Luminescent polynuclear metal acetylides. J Organomet Chem 578:3–30
16. Yam VW-W, Lee WK, Cheung K-K, Crystall B, Phillips D (1996) Synthesis, structure, photophysics, time-resolved emission spectroscopy and electrochemistry of luminescent copper(I) acetylide complexes. J Chem Soc Dalton Trans. 3283–3287. doi:1039/DT9960003283
17. Wong E, Li J, Seward C, Wang S (2009) Cu(I) and Ag(I) complexes of 7-azaindolyl and 2,2'-dipyridylamino substituted 1,3,5-triazine and benzene: the central core impact on structure, solution dynamics and fluorescence of the complexes. Dalton Trans 14:1776–1785
18. McCormick T, Jia W-L, Wang S (2006) Phosphorescent Cu(I) complexes of 2-(2′-pyridylbenzimidazolyl)benzene: impact of phosphine ancillary ligands on electronic and photophysical properties of the Cu(I) complexes. Inorg Chem 45:147–155
19. Zhang L, Li B, Su ZM (2009) Realization of high-energy emission from [Cu(N-N)(P-P)] + complexes for organic light-emitting diode applications. J Phys Chem C 113:13968–13973
20. Yu TZ, Wang ZY, Zhao YL, Wen XG, Zhang H, Fan DW (2012) Synthesis, crystal structure and photoluminescence of phosphorescent copper (I) complexes containing hole-transporting carbazolyl group. Inorg Chim Acta 383:78–82
21. Yu TZ, Chai HF, Zhao YL, Zhang CC, Liu P, Fan DW (2013) Synthesis, crystal structure and photoluminescence of phosphorescent copper(I) complexes containing hole-transporting carbazoly moiety. Spectrochim Acta A Mol Biomol Spectrosc 109:179–185
22. Hsu CW, Lin CC, Chung MW, Chi Y, Lee GH, Chou PT, Chang CH, Chen PY (2011) Systematic investigation of the metal-structurephotophysics relationship of emissive d^{10}-complexes of group 11 elements: the prospect of application in organic light emitting devices. J Am Chem Soc 133:12085–12099
23. Wada A, Zhang QS, Yasuda T, Takasu I, Enomoto S, Adachi C (2012) Efficient luminescence from a copper(I) complex doped in organic light-emitting diodes by suppressing C-H vibrational quenching. Chem Commun 48:5340–5342
24. Deaton JC, Switatski SC, Kondakov DY, Young RH, Pawlik TD, Giesen DJ, Harkins SB, Miller AJM, Mickenberg SF, Peters JC (2010) E-type delayed fluorescence of a phosphine-supported $Cu_2(\mu\text{-}Nar_2)_2$ diamond core: harvesting singlet and triplet excitons in OLEDs. J Am Chem Soc 132:9499–9508
25. Hashimoto M, Igawa S, Yashima M, Kawata I, Hoshino M, Osawa M (2011) Highly efficient green organic light-emitting diodes containing luminescent three-coordinate copper(I) complexes. J Am Chem Soc 133:10348–10351
26. Zhang QS, Ding JQ, Cheng YX, Wang LX, Xie ZY, Jing XB, Wang FS (2007) Novel heteroleptic Cu^I complexes with tunable emission color for efficient phosphorescent light-emitting diodes. Adv Funct Mater 17:2983–2990
27. Zhang QS, Zhou QG, Cheng YX, Wang LX, Ma DG, Jing XB, Wang FS (2004) Highly efficient green phosphorescent organic light-emitting diodes based on Cu(I) complexes. Adv Mater 16:432–436
28. Yu TZ, Meng J, Zhao YL, Zhang H, Han XQ, Fan DW (2011) Synthesis and rare earth metal ion-sensing properties of aza-crown derivative incorporating with diaryl-1,3,4-oxadiazole. Spectrochim Acta Part A Mol Biomol Spectrosc 78:396–400
29. Kubas GJ (1979) Tetrakis(acetonitrile)copper(I) hexafluorophosphate. Inorg Synth 19:90–92
30. Cuttell DG, Kuang SM, Fanwick PE, McMillin DR, Walton RA (2002) Simple Cu(I) complexes with unprecedented excited-state lifetimes. J Am Chem Soc 124:6–7
31. Zhang LM, Li B, Su ZM (2009) Phosphorescence enhancement triggered by π stacking in solid-state [Cu(N−N)(P−P)]BF4 complexes. Langmuir 25:2068–2074
32. Kupka H, Ensslin W, Wernicke R, Schmidtke H (1979) Intensity distribution in the progressions of vibronic transitions of metal-ion complexes. Mol Phys 37:1693–1701
33. Czerwieniec R, Yu J, Yersin H (2011) Blue-light emission of Cu(I) complexes and singlet harvesting. Inorg Chem 50:8293–8301
34. Zink DM, Bächle M, Baumann T, Nieger M, Kühn M, Wang C, Klopper W, Monkowius U, Hofbeck T, Yersin H, Bräse S (2013) Synthesis, structure, and characterization of dinuclear copper(I) halide complexes with P^N ligands featuring exciting photoluminescence properties. Inorg Chem 52:2292–2305

Supplementary material

The crystallographic data (excluding structure factors) of the ligand L and $[Cu(L)(PPh_3)_2](BF_4)\bullet 2CH_2Cl_2$ had been deposited with the Cambridge Crystallographic Data Center as supplementary publication no. CCDC 943611 and 943612, respectively.